

BASIC SCIENCE

Mechanical properties of the drug-eluting bioresorbable magnesium scaffold compared with polymeric scaffolds and a permanent metallic drug-eluting stent

Trine Ø. Barkholt MD¹  | Bruce Webber MHSc² | Niels R. Holm MD¹ | John A. Ormiston MBChB^{2,3}

¹Aarhus University Hospital, Aarhus, Denmark

²Intra, Auckland, New Zealand

³University of Auckland, Auckland, New Zealand

Correspondence

Trine Ø. Barkholt, Department of Cardiology, Aarhus University Hospital, Palle Juul-Jensens Boulevard 99, 8200 Aarhus, Denmark.
Email: trio@clin.au.dk

Funding information

Biotronik, Grant/Award Number: Scaffolds for testing were provided

Abstract

Objectives: To compare on the bench the physical and mechanical properties of Magmaris, a magnesium bioresorbable scaffold (BRS), with Absorb and DESolve polymeric BRS and a permanent metallic stent.

Background: Understanding the mechanical and physical properties of BRS is crucial for appropriate implantation and postdilatation.

Methods: Testing was performed in fluid at 37°C and in silicone bifurcation phantoms with a 30° angle between main branch (MB) and side branch.

Results: The 3.0-mm Magmaris BRS did not fracture after MB postdilatation up to 4.4 mm in contrast to the Absorb where the safe postdilatation diameter was 3.7 mm. For dilatation through stent cells, there were no Magmaris fractures with 3.0-mm noncompliant (NC) balloons inflated to nominal pressure. Mini-kissing balloon postdilatation with two 3.0-mm NC balloons up to 17 atm was without fracture except for an outlier. Longitudinal and radial strengths were similar for Magmaris and Absorb BRS. The crossing profile for the Magmaris was larger than other devices. Recoil 120 min after deployment was the greatest for Magmaris but 120 min after 3.5 mm postdilatation all devices had similar diameters.

Conclusions: The Magmaris BRS was more resistant to strut fracture than Absorb. It had a larger crossing profile than other devices and similar radial and longitudinal strengths to Absorb. While recoil after deployment was greater with Magmaris, 120 min after 3.5 mm postdilatation all devices had similar diameters.

KEYWORDS

bifurcations, bioresorbable scaffolds, mechanical properties, percutaneous coronary intervention, stent, stenting technique, strut fracture

1 | INTRODUCTION

Permanent metallic drug-eluting stents (DES) have a late incidence of adverse events of a few percent annually indefinitely. It is hoped that full resorption of a bioresorbable scaffold (BRS) will reduce this.¹⁻³

Current BRSs have important limitations including inferior deliverability, lower radial strength, lower expansion capacity, and higher rates of scaffold thrombosis when compared with permanent DES.⁴⁻⁷ As different BRS platforms have different properties, the interventional cardiologist needs to be aware of these differences to ensure safe

This is an open access article under the terms of the Creative Commons Attribution-NonCommercial-NoDerivs License, which permits use and distribution in any medium, provided the original work is properly cited, the use is non-commercial and no modifications or adaptations are made.

© 2019 The Authors. *Catheterization and Cardiovascular Interventions* published by Wiley Periodicals, Inc.

and effective deployment. The magnesium-based Magmaris BRS (Biotronik AG, Bülach, Switzerland) has shown promising results in recent trials^{8,9} Mechanical properties of the Magmaris magnesium alloy are closer to permanent metallic DES than those of poly-L-lactic acid (PLLA) scaffolds, and this may be reflected in improved properties of the Magmaris over PLLA scaffolds.

In this study, we compared the mechanical properties of the Magmaris BRS with the Absorb (Abbott Vascular, Santa Clara, CA) and DESolve BRS (Elixir Medical Corporation, Sunnyvale, CA) and with the permanent metallic DES MultiLink8 (ML8)/Xience Xpedition (Abbott Vascular). Our focus was on safe postdilatation thresholds and side branch (SB) dilatation strategies. We compared our Magmaris results with those for Absorb, DESolve, and Xience using the same methodology.¹⁰⁻¹²

2 | MATERIALS AND METHODS

2.1 | Scaffolds and stents

The Magmaris BRS is a sirolimus-eluting magnesium alloy scaffold and is the first metallic BRS in clinical use. The alloy degrades to magnesium hydroxide, magnesium phosphate, and amorphous calcium phosphate. The degradation process is relatively fast compared with other BRS with 95% of the magnesium resorbed after 12 months. The design of the scaffold is in-phase sinusoidal hoops with two connectors per hoop linking valleys and peaks (Figure 1). There are two radiopaque tantalum markers at each end. The strut thickness and width are 150 μm for the 3.0-mm scaffold.¹³

The Absorb BRS was everolimus-eluting and constructed from PLLA. It had in-phase sinusoidal hoops with six peaks and valleys per hoop and three connectors. The strut thickness including polymer coating was 157 μm , the hoop width was 191 μm , and the connector width 140 μm for the 3.0-mm scaffold (Figure 1).¹⁰ Absorption time was around 3–4 years.

The DESolve 150 BRS is a novolimus-eluting PLLA-based scaffold with a resorption time of 1–2 years. The design is sinusoidal hoops with nine peaks and valleys and three connectors per hoop. Strut thickness including polymer coating is 150 μm . Hoop width is 165 μm and connector width 100 μm (Figure 1).¹⁰

The DESolve Cx is also a novolimus-eluting PLLA-based scaffold with a similar design but thinner hoops at 120 μm (Figure 1).

The ML8 is the bare metal platform of the everolimus-eluting Xience Xpedition DES. It is constructed from cobalt chromium with in-phase sinusoidal hoops. Each hoop has six peaks and valleys and three connectors. Strut thickness including the polymer coating according to the manufacturer is 89 μm (Figure 1).

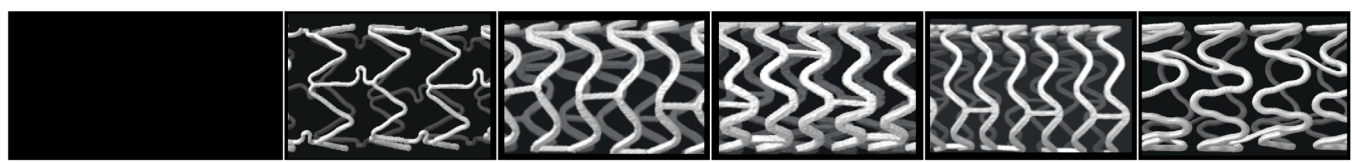
2.2 | Bench test setup

Bench testing of the Magmaris BRS in this study is compared with the previously published results for Absorb, DESolve 150, and ML8.¹⁰⁻¹²

Tests were performed in a 37°C simulated body fluid (SBF) bath except for SB dilatation, which were performed in a 37°C water bath. Crossing profile was measured in air.

Deployments and postdilatations were recorded fluoroscopically. Photographs were recorded with an EOS-5D Canon digital camera (Canon, Inc., Tokyo, Japan) and a Leica Z6 APO microscopic lens (Leica Microsystems, Wetzlar, Germany). All measurements were performed on photographs using the Image Pro Plus software (Version 7.0.0.591 Media Cybernetics, Inc., Bethesda, MD). Calibration was performed before each measurement. Selected scaffolds were imaged by micro-CT (SkyScan1172, Sky-Scan, Belgium). All balloon dilatations were performed using noncompliant (NC) balloons.

The number of devices for each design (3.0 mm nominal diameter) in each test is shown in Table 1.



Device	ML8/Xience Xpedition	Absorb	Desolve	Desolve Cx	Magmaris
Strut thickness, μm	89	157	150	120	150
Strut width, μm	Hoop 89-112	Hoop 191 Connector 140	Hoop 165 Connector 100	Hoop 165 Connector 100	Hoop 150 Connector 80-100
Strut coverage, % (strut coverage of vessel wall footprint) at nominal size)	13	27	30	30	20

FIGURE 1 Comparison of strut dimensions and vessel coverage for bioresorbable and permanent stents. Measurements provided by manufacturers

	Magmaris	Absorb	DESolve	DESolve cx	Xience/ML8
Crossing profile	10	6	5	5	3
Recoil	10	10	5	5	5
Main branch postdilatation	11	13	5	5	2
Side branch dilatation	10	24	14	9	5
Mini-kissing postdilatation	5	10	4	5	5
Radial strength	5	5	—	—	5
Longitudinal strength	5	5	—	—	5

Abbreviation: ML8, MultiLink8.

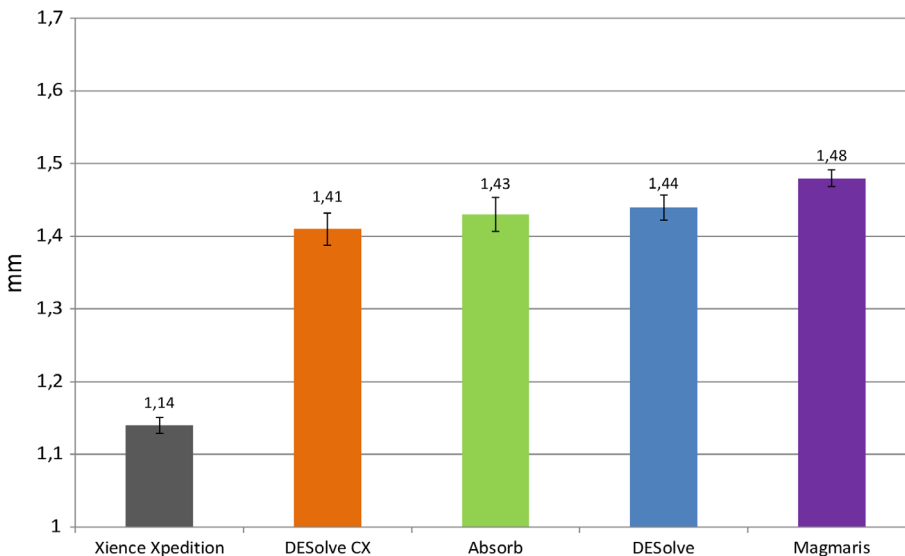


TABLE 1 Number of devices of each design for each test

FIGURE 2 Crossing profiles. The crossing profiles (mm) of bioresorbable scaffolds and a permanent metallic drug-eluting stent are shown

2.3 | Scaffold crossing profile

The devices were photographed in air from two orthogonal projections. Crossing profile was measured as the diameter of the undeployed scaffold mounted on the delivery system.

2.4 | Recoil

Recoil was the percentage change in device diameter measured on the inflated balloon at nominal pressure and after balloon deflation (Figure 3). The scaffold was in SBF for 1 min before unconstrained deployment at nominal pressure. One minute after deployment, the scaffold was removed from the bath, without being deflated and was photographed for diameter measurements. The scaffold was then returned to the bath before deflation. Measurements were performed 1 and 10 min after deflation. After 10 min, the devices were separated into two groups. Group 1 underwent postdilatation with a 3.5-mm NC balloon at nominal pressure and was measured immediately and at 1 and 10 min and at 1 and 2 hr. Group 2 was measured postdeployment at 1 and 10 min and at 1 and 2 hr before postdilatation. After postdilatation measurements were performed at 1 and 10 min. The results for postdilatation measurements at 1 and 10 min were pooled from the two groups as device diameters were stable 10 min after deployment (Figure 3).

2.5 | Phantom design

These were three-dimensional (3D) printed in with a 30° angle B between the main branch (MB) and the SB.¹⁴ The diameter of the proximal MB was 3.5 mm, distal MB was 3.0 mm, and SB was 3.0 mm.

2.6 | MB postdilatation and strut fracture

Devices unconstrained in an SBF bath at 37°C were postdilated to 18 atm with increasing diameter balloons (3.5, 4.0, 4.5, and 5.0 mm) or until strut fracture. Photographs were taken at every 2 atm pressure increase to document fracture. When fracture occurred, the scaffold and balloon were removed from the bath and rephotographed for diameter measurements. The percentage of scaffolds with fracture was plotted against balloon diameter (Figure 4).

2.7 | SB dilatation

Evaluation of balloon inflation into the SB through scaffold/stent cells after MB implantation was performed under fluoroscopic control in a 37°C water bath. Scaffolds and stents with a nominal diameter of 3.0 mm were deployed in the MB of the silicone phantoms. Proximal optimization technique (POT) was performed using 3.5-mm NC balloons with slow inflation at approximately 2 atm/s to nominal pressure. The SB was dilated with increasing balloon diameters (2.0, 2.5, and to 3.0 mm) at

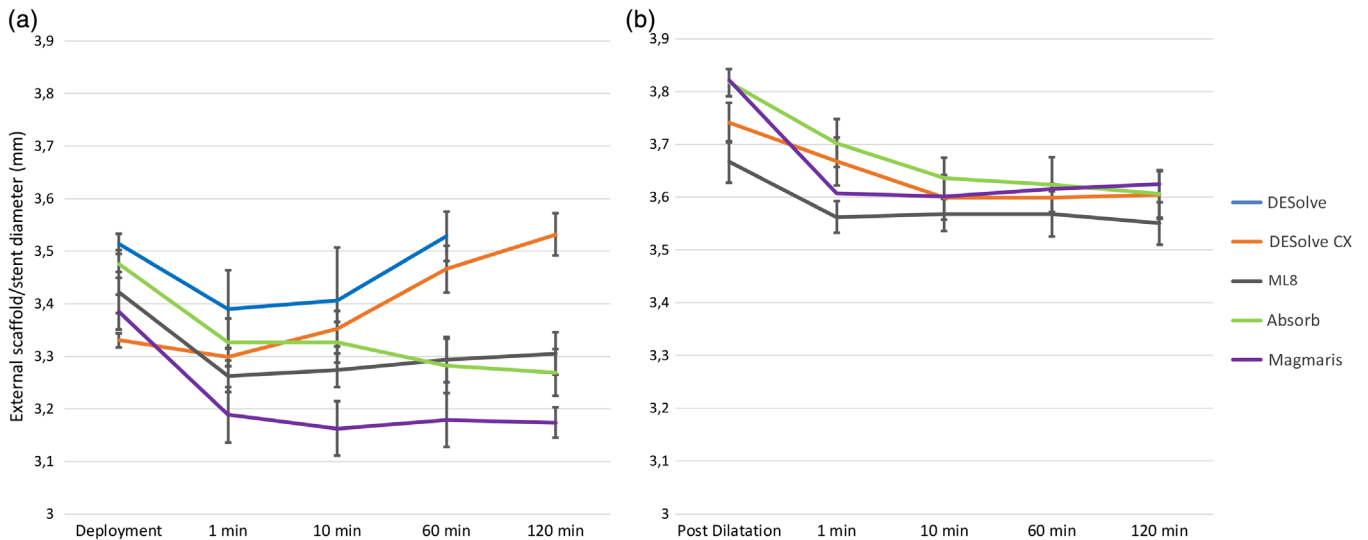


FIGURE 3 Recoil after deployment and after postdilatation. (a) Recoil assessed by measuring the external diameter of 3.0-mm scaffolds/stents at deployment and over 2 hr following balloon deflation is plotted. The diameter seems stable 10 min after inflation except for DESolve, which is known for self-expansion. (b) Recoil of devices over 2 hr following postdilatation with a 3.5-mm noncompliant balloon at 12 atm. Half of the devices were postdilated 10 min after inflation and the other half after 2 hr. The results for 1 and 10 min after postdilatation were pooled as measurements were stable after 10 min. While Magmaris had the greatest recoil over the 2 hr following deployment, at the end of 2 hr following postdilatation, all devices had similar external diameters

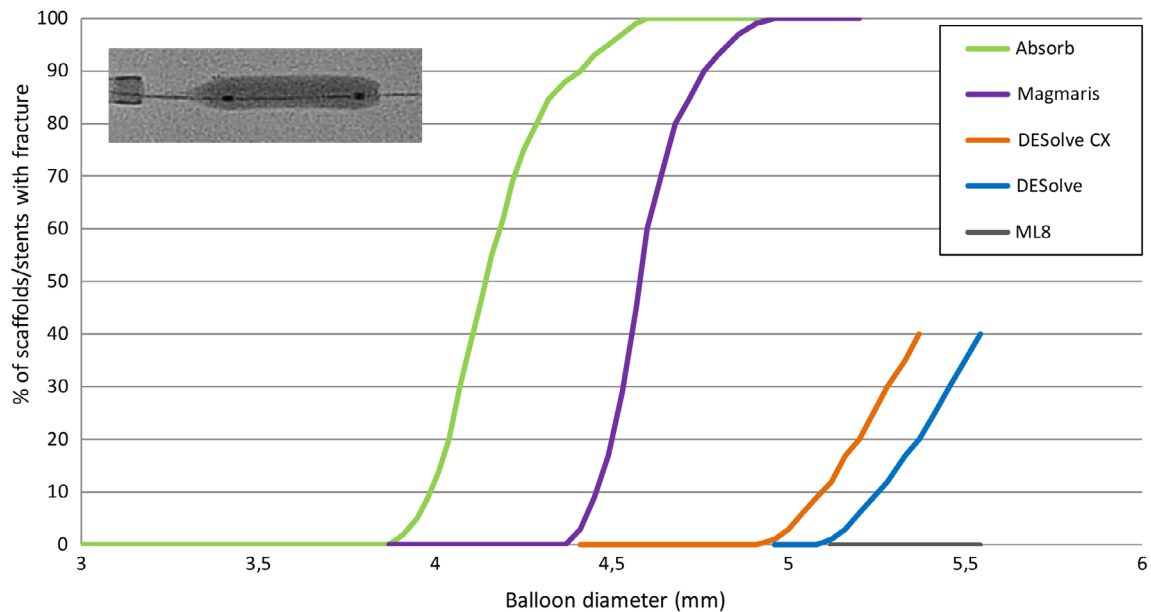


FIGURE 4 Scaffold strut fracture and balloon diameter. Percentage of 3.0-mm scaffolds with fracture with increasing main branch balloon diameter

14 atm. If no fractures were observed, the 3.0-mm balloon was inflated to 18 and 22 atm. The scaffolds were observed for strut fracture at each incremental step in pressure. Images were recorded by both fluoroscopy and photography (Figure 5a).

2.8 | Mini-kissing balloon postdilatation and strut fracture

Mini-kissing balloon postdilatation (Mini-KBPD) refers to simultaneous inflation of a balloon in the MB and an SB balloon that protrudes only a

few millimeters into the proximal MB.¹¹ Mini-KBPD was performed in phantoms of the same design as above using two 3.0-mm NC balloons that were inflated slowly and simultaneously until fracture was observed or 20 atm pressure achieved (Figure 5b).

2.9 | Radial strength

The radial strength of the stents and scaffolds was measured by the cross-sectional area reduction of an expanded device exposed to increasing external pressure at 0.1 mmHg increments in a 37°C SBF

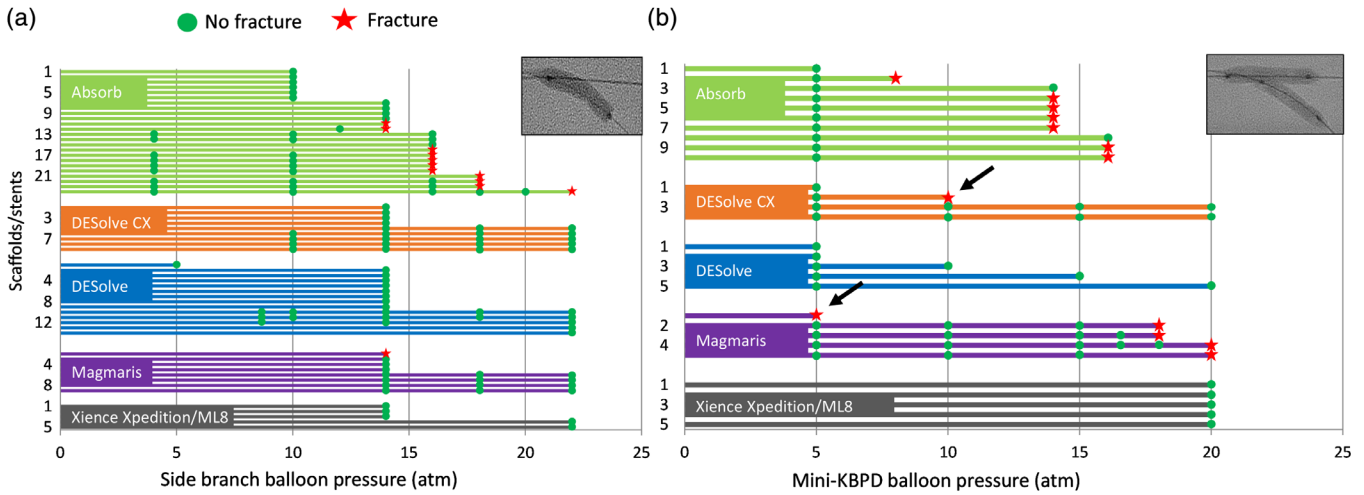


FIGURE 5 Scaffold fracture with SB dilatation and with mini-KBPD. On the horizontal axis is balloon pressure and on the vertical axis different devices. The red stars indicate strut fractures, and green dots indicate the pressures where inspections were made and where there were no fractures. Black arrows indicate outliers. (a) Strut fracture in individual scaffolds or stents dilated through a cell toward the SB with a 3.0-mm balloon. (b) Strut fracture after mini-KBPD with two 3.0-mm balloons at increasing pressures. Mini-KBPD means simultaneous inflation of a balloon in the MB and a balloon in the SB with minimal overlap of these balloons in the MB. MB, main branch; mini-KBPD, mini-kissing balloon postdilatation; SB, side branch

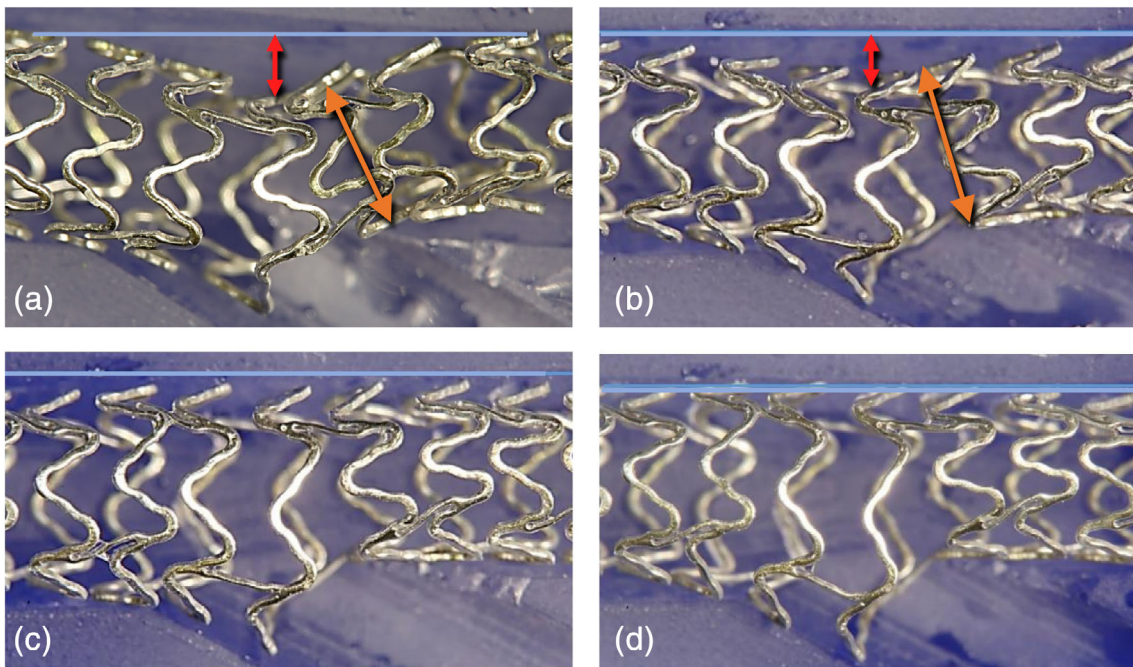


FIGURE 6 Magmaris scaffold distortion after SB dilatation and correction with mini-KBPD. (a) A 3.0-mm Magmaris bioresorbable scaffold after SB dilatation with a 3.0-mm noncompliant balloon at 14 atm is distorted. Notice the malapposition (double-headed red arrows) opposite to the SB and metallic narrowing (double-headed yellow arrow) just distal to the SB. (b) Mini-KBPD at 5 atm partially corrects the malapposition and narrowing. (c) Mini-KBPD at 10 atm was the lowest pressure to correct distortion. (d) Mini-KBPD at 15 atm. mini-KBPD, mini-kissing balloon postdilatation; SB, side branch

bath. An Intravascular ultrasound (IVUS) catheter within the scaffold or stent measured cross-sectional area loss with the Clearview IVUS quantitative analysis, which was plotted against increasing pressure. Pressures required to reduce cross-sectional area by 10 and 25% and to cause collapse were plotted (Figure 7).

2.10 | Longitudinal strength

Longitudinal strength was assessed with an Instron 5866 Universal Testing Machine employing a previously published setup.¹² Devices were deployed in the testing rig with proximal malapposition. A hypotube was lowered to touch the valley of the proximal hoop

(Figure 8). The scaffold was compressed to 4 mm in 37°C SBF with a stop each 1 mm for photography while the Instron recorded force applied in Newtons.

2.11 | Statistics

Descriptive statistics are presented as mean \pm SD or as counts (%). Differences in categorical variables were analyzed using the Fisher's exact test and differences in continuous variables by the Mann-Whitney test. A p value of .05 was considered significant. All p values

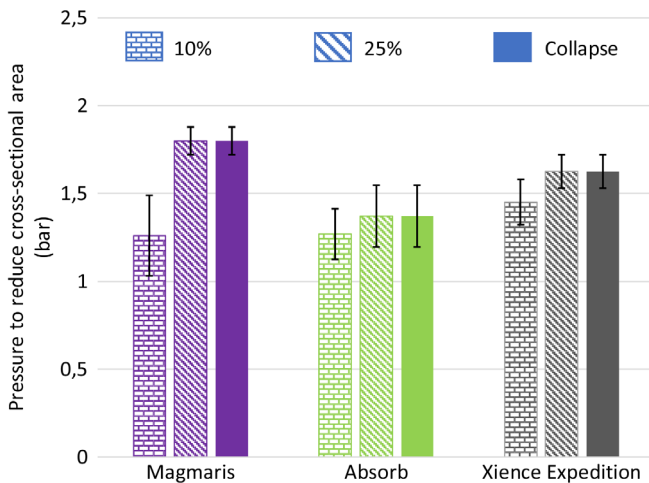


FIGURE 7 Scaffold radial strength. This is depicted as the pressure to reduce device cross-sectional area by 10 and 25% and to cause device collapse

resulted from two-sided tests. Statistical analyses were performed using the Microsoft Excel or STATA (version 12; StataCorp LLC, Texas).

3 | RESULTS

3.1 | Crossing profile

The crossing profile of the Magmaris BRS (1.48 ± 0.01 mm) was larger than Absorb BRS (1.43 ± 0.02 mm) and ML8 permanent stent (1.14 ± 0.01 mm), $p = .01$ and $p = .01$, respectively (Figure 2).

3.2 | Recoil

Stent and scaffold diameters seemed stable 10 min (min) after inflation (Figure 3a), except for the DESolve device which is known to self-expand. Recoil measured 120 min after deployment was the largest in the Magmaris and Absorb BRS but postdilatation with a 3.5-mm balloon at nominal pressure, while there was some recoil with all devices, external diameters were greater when compared with the strategy of inflating to nominal pressure without postdilatation. Resulting external device diameters 120 min after postdilatation of Magmaris and Absorb BRS were similar at 3.62 ± 0.03 and 3.61 ± 0.02 mm, respectively, $p = .35$ (Figure 3).

3.3 | MB postdilatation and strut fracture

The 3.0-mm Magmaris BRS did not fracture during postdilatation with balloon diameters up to 4.4 mm, and we observed no fractures with

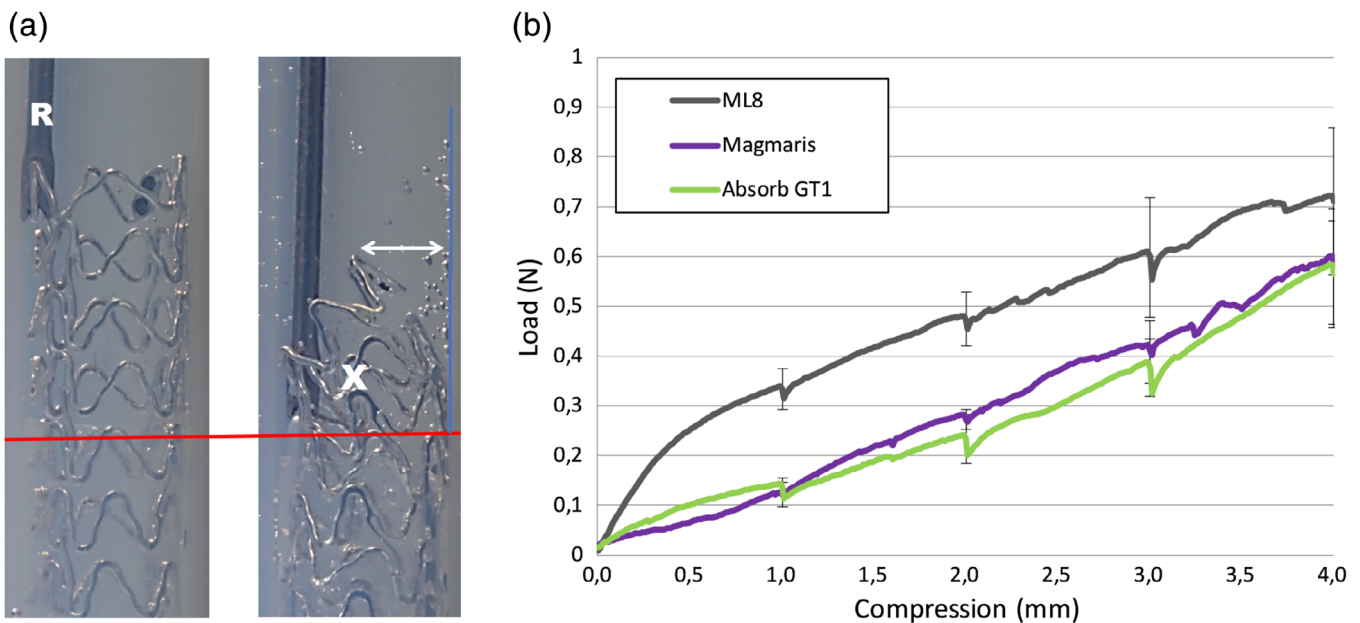


FIGURE 8 Point longitudinal compression testing. (a) Force is applied to a point on the most proximal hoop of the Magmaris bioresorbable scaffold by a rod (R) attached to an Instron. Hoops were pushed together (X) on that side of the lumen, and malapposition was prominent on the opposite side (double-headed arrow). (b) Point compression up to 4.0 mm for four stents/scaffolds. With compression up to 3.0 mm, the Magmaris and Absorb showed less longitudinal strength than the MultiLink 8

postdilatation with a 4.0-mm NC balloon at any pressure. Compared with other BRS, the Magmaris was less likely to fracture than the Absorb but more likely than the DESolve (Figure 4). All Magmaris fractures after MB postdilatation were in scaffold hoops.

3.4 | SB dilatation

We observed no fractures with inflation of 3.0-mm SB balloons up to 22 atm, except for one outlier, which occurred at a pressure less than 14 atm (Figure 5a). This outlier fracture was in a connector at its junction with the hoop and was likely caused by a damaged balloon tip catching on the strut during difficult passage of the balloon through the side of the scaffold.

3.5 | Mini-KBPD, strut fracture, and correction of distortion

With mini-KBPD of the Magmaris with two 3.0-mm balloons, all fractures occurred at 18 atm or more except for one unexplained outlier at 5 atm (Figure 5b). All these fractures were at the junction of connector and hoop. Distortion of the scaffold due to SB dilatation (malapposition opposite to the SB and metallic narrowing in the scaffold distal to the SB) was abolished with mini-KBPD pressure at 10 atm or more (Figure 6).

3.6 | Radial strength

The pressure required to reduce the cross-sectional area of the Magmaris scaffold by 10% was similar to that of Absorb (1.26 ± 0.23 vs. 1.27 ± 0.14 bar, $p = .67$). The pressure needed to reduce Magmaris by 25% was greater than that for Absorb (1.8 ± 0.08 vs. 1.37 ± 0.18 bar, $p = .01$) (Figure 7).

3.7 | Longitudinal strength

The force applied by the rod causing 4-mm compression resulted in scaffold hoops being pushed together, obstructing the lumen and dragging opposite struts in toward the lumen causing malapposition. We found no difference in the force required to compress the scaffold 4 mm when comparing Magmaris and Absorb BRS (0.58 ± 0.12 and 0.56 ± 0.11 N, $p = .75$). The ML8 required numerically higher pressures (0.71 ± 0.15 N); however, this did not reach statistical significance ($p = .08$).

4 | DISCUSSION

In this bench study of the 3.0-mm Magmaris BRS compared with previously tested scaffolds and stents, the main findings were as follows:

1. MB postdilatation with balloon diameters less than 4.4 mm did not cause fracture.
2. SB dilatation with a 3.0-mm balloon up to 22 atm did not cause fracture except for one outlier at 14 atm.

3. Mini-KBPD with two 3.0-mm balloons was safe with pressures up to 18 atm, except for a single outlier at 5 atm. Mini-KBPD at 10 atm or more corrected distortion after SB dilatation.

4. Radial strength (pressure to reduce cross-sectional area by 10%) was similar for Magmaris and Absorb. For 25% reduction in cross-sectional area, Magmaris required a greater pressure than Absorb and hence had greater radial strength.

5. Magmaris had more acute recoil after deployment than Absorb, but 120 min after postdilatation with a 3.5 mm NC balloon, the diameters of devices were similar.

Concerns about late outcomes with durable metallic DES prompted the development of BRS that leaves no foreign material in the coronary artery after a scaffold-specific resorption time. Absorb BRS was the first fully bioresorbable device evaluated in randomized trials powered for clinical outcome.^{10,11,15-18} The crossing profile of the Absorb reduced its deliverability with less device success than durable DES in randomized trials.^{15,16,19} The Absorb had a higher rate of thrombosis than contemporary durable metallic DES.^{4,20} Possible causes include implantation in small diameter vessels, under expansion, intraluminal strut degradation, and loss of radial strength or fracture leading to scaffold detachment or collapse. In addition, the scaffold strut thickness and width along with the relatively large volume of foreign material likely caused increased platelet activation and predisposed to stent thrombosis.²¹

The Magmaris BRS was evaluated in the BIOSOLVE studies and showed good clinical results and no definite scaffold thrombosis.^{9,22} The magnesium alloy has mechanical properties that are somewhat closer to cobalt chromium compared with PLLA used as the Absorb backbone. Thrombogenicity of the Magmaris is lower than that for Absorb BRS.^{23,24}

Our bench evaluation of Magmaris BRS showed higher expansion capacity without scaffold fracture compared with Absorb both in the main lumen and through the side of the scaffold. The outliers where Magmaris fractured at low balloon pressures (Figure 5) may be related to the position of the rewired cell across the SB ostium. If the rewired cell is only partly across the SB ostium, it is possible that struts are trapped and unable to move with the balloon expansion resulting in fracture.²⁵ The DESolve BRS and the ML8/Xience Xpedition did not fracture during SB dilatation or mini-KBPD.

The stent distortion observed after SB dilatation occurs with all devices.²⁶ Mini-KBPD corrected distortion without losing the positive aspects of SB dilatation, specifically the SB ostial size and protrusion of struts into the SB (Figure 6). The fractures after mini-KBPD were single connectors and were minimally displaced without luminal protrusion and unlikely to have clinical significance. Single connector fractures are less likely to be detected by 2D IVUS or 2D OCT and even by 3D OCT due to minimal displacement of fractured ends.²⁷ An in vivo bifurcation study performed with implantations in rabbits found no scaffold fractures by the provisional approach with predilatation, POT, SB opening, and KBPD strategies.²⁷

A major limitation of the Absorb BRS was increased rates of scaffold thrombosis.^{4,7} Magmaris has a smaller footprint within the artery than Absorb. The percentage vessel coverage for a 3.0-mm device

was 20% for Magmaris and was 27% for Absorb. In addition, the Magmaris struts are thinner and narrower (Figure 1). These features along with the lower thrombogenicity of the magnesium alloy may lead to a lower incidence of scaffold thrombosis for Magmaris. However, large clinical studies with Magmaris would be required to determine this.

Achieving sufficient acute radial strength while keeping strut thickness and width as small as possible is a design challenge for BRS. Magmaris has higher radial strength than Absorb but less compared with permanent metallic stents. The evaluated scaffolds showed differences in recoil over the first 2 hr with a rather large loss by Magmaris when delivered at nominal pressure. Routine postdilatation of the 3.0-mm Magmaris with a 3.5-mm NC balloon countered this difference so that there was little difference between all evaluated devices after 2 hr (Figure 3).

5 | LIMITATIONS

Bench tests of devices may not predict clinical performance. The phantoms in which devices were deployed were disease free, and elasticity may not be similar to human arteries. The number of tested scaffolds and stents of each design was limited thus affecting power of statistical comparison. As data were collected at different timepoints, this could potentially cause variations in test conditions. Still, tests were performed using the same protocol and testing equipment, in the same laboratory by the same personnel. The results apply to the tested scaffolds and do not apply to other BRS.

6 | CONCLUSIONS

The mechanical properties of the Magmaris BRS were superior to the Absorb BRS but inferior to durable metallic stents. The acute recoil with a 3.0-mm Magmaris was countered with routine postdilatation with a 3.5-mm balloon. For Magmaris, postdilatation of a scaffold with a balloon up to 4.4 mm diameter was safe. SB dilatation up to 14 atm was generally safe as was mini-KBPD up to 15 atm. Stent and scaffold distortion due to SB dilatation can be corrected by mini-KBPD at 10 atm.

ACKNOWLEDGMENTS

The data on Absorb, DESolve, and Xience were previously published.¹⁰⁻¹² Figures 2, 3, 4, 5, and 7 are amended with new data on Magmaris and DESolve Cx and reprinted from *EuroIntervention* 2015/ Vol 11, John A. Ormiston, Bruce Webber, Ben Ubod, Olivier Darremont, Mark W.I. Webster, An independent bench comparison of two bioresorbable drug-eluting coronary scaffolds (Absorb and DESolve) with a durable metallic drug-eluting stent (ML8/Xpedition), Page 60-7, 2015, with permission from Europa Digital & Publishing. The study was supported by Biotronik with investigators having full control of the data.

CONFLICT OF INTERESTS

T.Ø.B. and B.W. declare no conflict of interests. N.R.H.: Institutional research grants and speaker fees from Abbott, Biotronik, Boston Scientific, and Reva Medical. J.A.O.: Advisory Board and minor honoraria from Boston Scientific.

ORCID

Trine Ø. Barkholt  <https://orcid.org/0000-0002-7415-6724>

REFERENCES

- Brugaletta S, Radu MD, Garcia-Garcia HM, et al. Circumferential evaluation of the neointima by optical coherence tomography after ABSORB bioresorbable vascular scaffold implantation: can the scaffold cap the plaque? *Atherosclerosis*. 2012;221:106-112.
- Ormiston JA, Serruys PW, Regar E, et al. A bioabsorbable everolimus-eluting coronary stent system for patients with single de-novo coronary artery lesions (ABSORB): a prospective open-label trial. *Lancet*. 2008; 371:899-907.
- Serruys PW, Garcia-Garcia HM, Onuma Y. From metallic cages to transient bioresorbable scaffolds: change in paradigm of coronary revascularization in the upcoming decade? *Eur Heart J*. 2012;33:16-25b.
- Wykrzykowska JJ, Kraak RP, Hofma SH, et al. Bioresorbable scaffolds versus metallic stents in routine PCI. *N Engl J Med*. 2017;376:2319-2328.
- Cassese S, Byrne RA, Juni P, et al. Midterm clinical outcomes with everolimus-eluting bioresorbable scaffolds versus everolimus-eluting metallic stents for percutaneous coronary interventions: a meta-analysis of randomised trials. *EuroIntervention*. 2018;13:1565-1573.
- Cassese S, Byrne RA, Ndrepepa G, et al. Everolimus-eluting bioresorbable vascular scaffolds versus everolimus-eluting metallic stents: a meta-analysis of randomised controlled trials. *Lancet*. 2016; 387:537-544.
- Capodanno D, Gori T, Nef H, et al. Percutaneous coronary intervention with everolimus-eluting bioresorbable vascular scaffolds in routine clinical practice: early and midterm outcomes from the European multicentre GHOST-EU registry. *EuroIntervention*. 2015;10:1144-1153.
- Haude M, Ince H, Abizaid A, et al. Safety and performance of the second-generation drug-eluting absorbable metal scaffold in patients with de-novo coronary artery lesions (BIOSOLVE-II): 6 month results of a prospective, multicentre, non-randomised, first-in-man trial. *Lancet*. 2016;387:31-39.
- Haude M, Ince H, Abizaid A, et al. Sustained safety and performance of the second-generation drug-eluting absorbable metal scaffold in patients with de novo coronary lesions: 12-month clinical results and angiographic findings of the BIOSOLVE-II first-in-man trial. *Eur Heart J*. 2016;37:2701-2709.
- Ormiston JA, Webber B, Ubod B, Darremont O, Webster MW. An independent bench comparison of two bioresorbable drug-eluting coronary scaffolds (Absorb and DESolve) with a durable metallic drug-eluting stent (ML8/Xpedition). *EuroIntervention*. 2015;11: 60-67.
- Ormiston JA, Webber B, Ubod B, Webster MW, White J. Absorb everolimus-eluting bioresorbable scaffolds in coronary bifurcations: a bench study of deployment, side branch dilatation and post-dilatation strategies. *EuroIntervention*. 2015;10:1169-1177.
- Ormiston JA, Webber B, Ubod B, White J, Webster MW. Stent longitudinal strength assessed using point compression: insights from a second-generation, clinically related bench test. *Circ Cardiovasc Interv*. 2014;7:62-69.

13. Fajadet J, Haude M, Joner M, et al. Magmaris preliminary recommendation upon commercial launch: a consensus from the expert panel on 14 April 2016. *EuroIntervention*. 2016;12:828-833.
14. Louvard Y, Thomas M, Dzavik V, et al. Classification of coronary artery bifurcation lesions and treatments: time for a consensus! *Catheter Cardiovasc Interv*. 2008;71:175-183.
15. Ellis SG, Kereiakes DJ, Metzger DC, et al. Everolimus-eluting bioresorbable scaffolds for coronary artery disease. *N Engl J Med*. 2015; 373:1905-1915.
16. Stone GW, Ellis SG, Gori T, et al. Blinded outcomes and angina assessment of coronary bioresorbable scaffolds: 30-day and 1-year results from the ABSORB IV randomised trial. *Lancet*. 2018; 392 (10157):1530-1540.
17. Foin N, Lee R, Bourantas C, et al. Bioresorbable vascular scaffold radial expansion and conformation compared to a metallic platform: insights from in vitro expansion in a coronary artery lesion model. *EuroIntervention*. 2016;12:834-844.
18. Serruys PW, Chevalier B, Sotomi Y, et al. Comparison of an everolimus-eluting bioresorbable scaffold with an everolimus-eluting metallic stent for the treatment of coronary artery stenosis (ABSORB II): a 3 year, randomised, controlled, single-blind, multicentre clinical trial. *Lancet*. 2016;388:2479-2491.
19. Stone GW, Gao R, Kimura T, et al. 1-year outcomes with the Absorb bioresorbable scaffold in patients with coronary artery disease: a patient-level, pooled meta-analysis. *Lancet*. 2016;387:1277-1289.
20. Yamaji K, Ueki Y, Souteyrand G, et al. Mechanisms of very late bioresorbable scaffold thrombosis: the INVEST registry. *J Am Coll Cardiol*. 2017;70:2330-2344.
21. Sotomi Y, Suwannasom P, Serruys PW, Onuma Y. Possible mechanical causes of scaffold thrombosis: insights from case reports with intracoronary imaging. *EuroIntervention*. 2017;12:1747-1756.
22. Haude M, Ince H, Kische S, et al. Sustained safety and clinical performance of a drug-eluting absorbable metal scaffold up to 24 months: pooled outcomes of BIOSOLVE-II and BIOSOLVE-III. *EuroIntervention*. 2017;13:432-439.
23. Waksman R, Lipinski MJ, Acampado E, et al. Comparison of acute thrombogenicity for metallic and polymeric bioabsorbable scaffolds: Magmaris versus Absorb in a porcine arteriovenous shunt model. *Circ Cardiovasc Interv*. 2017;10:e004762.
24. Lipinski MJ, Acampado E, Cheng Q, et al. Comparison of acute thrombogenicity for magnesium versus stainless steel stents in a porcine arteriovenous shunt model. *EuroIntervention*. 2018;14(13):1420-1427.
25. Barkholt TO, Ormiston JA, Ding P, et al. Coronary balloon catheter tip damage. A bench study of a clinical problem. *Catheter Cardiovasc Interv*. 2017;92(5):883-889.
26. Ormiston JA, Webster MW, Ruygrok PN, Stewart JT, White HD, Scott DS. Stent deformation following simulated side-branch dilatation: a comparison of five stent designs. *Catheter Cardiovasc Interv*. 1999;47:258-264.
27. Bennett J, Vanhaverbeke M, Vanden Driessche N, et al. The drug-eluting resorbable magnesium vascular scaffold in complex coronary bifurcations: insights from an in vivo multimodality imaging study. *EuroIntervention*. 2018;13:2036-2046.

How to cite this article: Barkholt TØ, Webber B, Holm NR, Ormiston JA. Mechanical properties of the drug-eluting bioresorbable magnesium scaffold compared with polymeric scaffolds and a permanent metallic drug-eluting stent. *Catheter Cardiovasc Interv*. 2020;96:E674–E682. <https://doi.org/10.1002/ccd.28545>